A Q-FACTOR ENHANCEMENT TECHNIQUE FOR MMIC INDUCTORS

Mina Danesh, John R. Long, R. A. Hadaway[1] and D. L. Harame[2]

University of Toronto
Toronto, Ontario, Canada

[1] Nortel Technology, Ottawa, Ontario, Canada
[2] IBM Microelectronics, Burlington, VT, USA

Abstract **- An increase of 50% in the peak Q-factor and a wider operating bandwidth for monolithic inductors is achieved by exciting a microstrip structure differentially. Conventional excitation of a 8 nH spiral inductor fabricated in a production silicon IC technology resulted in a peak (measured) Q-factor of 6.6 at 1.6 GHz, while the differential connection showed a maximum Q-factor of 9.7 at 2.5 GHz. These experimental results compared favorably with the behaviour predicted from simulation.**

I. INTRODUCTION

Microstrip inductors have been used extensively in radio frequency (RF) and monolithic microwave integrated circuits (MMIC). The quality factor (Q) of microstrip structures is limited by the series resistance of the metallization and, in the case of silicon technology, losses in the conductive substrate (typically 1 to 10 Ω-cm). The Q-factor is typically less than 10 for a metal-insulator-semiconductor (MIS) structure fabricated in a production silicon IC technology [1, 2]. It has been demonstrated that the quality factor can be improved by optimizing both the physical layout and structure of the inductor. Thicker metallization and stacking of metal layers reduces the conductor dissipation, thereby improving the Q [3]. Design guidelines have been proposed to optimize the geometric parameters of microstrip spiral inductors, such as strip width, spacing between the strips, and the gap between groups of coupled lines on opposing sides [1]. Losses in the semiconducting substrate may be reduced through the use of higher resistivity material [4], however, this is incompatible with current silicon device technology (e.g., CMOS). An alternative is to remove the underlying silicon by selective etching of the substrate or by applying a thin membrane beneath the inductor [5, 6], but this requires additional processing steps and there is a loss of mechanical strength when the underlying silicon is removed.

Microstrip spiral inductors are normally driven "single-ended", that is, the driving source is connected to one terminal of the spiral while the other end is grounded. Differential circuit topologies are common in integrated circuits, and consequently an alternative method that is practical for integrated circuits is to excite the spiral inductor differentially, using a source connected between the two ends of the microstrip spiral. The peak Q-factor shows a significant increase under differential excitation, and this high Q value is maintained over a broader bandwidth.

II. THEORY

A transmission line can be approximated over a range of frequencies by a lumped element equivalent circuit model. For a microstrip line fabricated in silicon technology, an appropriate equivalent circuit is shown in Fig. 1, where L is the total inductance of the line and r is the series resistance due to conductor losses and dissipation arising from current flowing in the silicon substrate. The shunt parasitics result from a combination of capacitances, due to an insulating layer of silicon dioxide (C_{ox}) and the underlying substrate (C_{si}), and substrate dissipation (R_{si}) [7]. For the spiral inductor, additional components are required to represent mutual magnetic and electric coupling between adjacent lines [1].

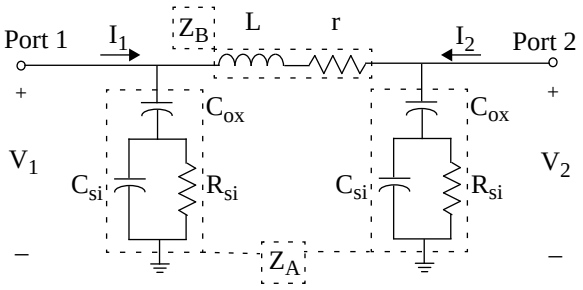

Fig. 1. Microstrip line equivalent circuit.

For single-ended excitation, Port 2 in Fig. 1 is grounded and the inductor is connected as a one-port. The input impedance at Port 1 (in this case Z_{SE}) becomes a parallel combination of two components: one due to the inductance and series dissipation (L and r in Fig. 1), the other due to the shunt R-C parasitic elements, as illustrated in Fig. 2. For a differential

0-7803-4471-5/98/$10.00 (c) 1998 IEEE

excitation, where the signal is applied between the two ports (i.e., between Port1 and Port2), the input impedance (Z_D) is due to the parallel combination of $2Z_A$ and Z_B, where impedances Z_A and Z_B are defined in Fig. 1. Since the substrate parasitics are connected together via the ground plane, the two shunt elements, are now in series (i.e., Z_A+Z_A), resulting in the equivalent circuit shown in Fig. 3.

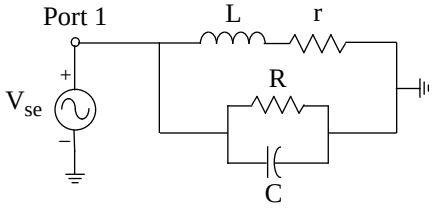

Fig. 2. Single-ended excitation model.

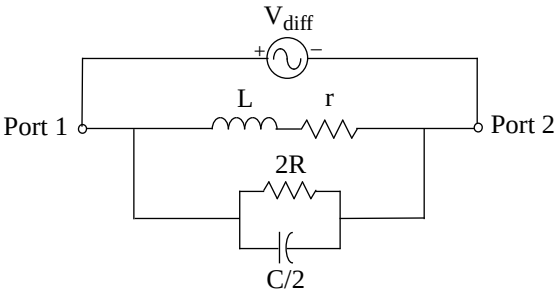

Fig. 3. Differential excitation model.

The quality factor of the inductor below the first resonant frequency is defined by

$$Q = \frac{2\pi fL}{Re[Z_{input}]} \quad (1)$$

where Z_{input} is the series equivalent input impedance. At lower frequencies, the input impedance in either the shunt or differential connections is approximately the same, but as the frequency increases, the substrate parasitics, C and R, come into play. For the case of differential excitation, these parasitics have a higher impedance at a given frequency than in the single-ended connection, as seen from comparison of Figs. 2 and 3. This reduces the real part and increases the reactive component of the input impedance. Therefore, the inductor Q-factor (from eq. 1) is improved when driven differentially, and moreover, a wider operating bandwidth can be achieved.

III. Analysis

A 5-turn square spiral inductor was fabricated and tested in order to verify these predictions. A cross-sectional view of a portion of the structure is illustrated in Fig. 4, and the substrate and metal properties for the fabrication process are listed in Table 1. The outer dimension, A, as shown in Fig. 5, is 250 μm. The inductor consists mainly of topmetal (M3) which is 8 μm wide and the spacing between conductors is 2.8 μm (w and s in Fig. 4, respectively). The relatively narrow conductor width and spacing results in higher magnetic coupling between microstrip lines and lower capacitive parasitics to the substrate. The inner gap between groups of coupled lines, G, is approximately 150 μm, which minimizes negative mutual coupling on opposite sides of the spiral.

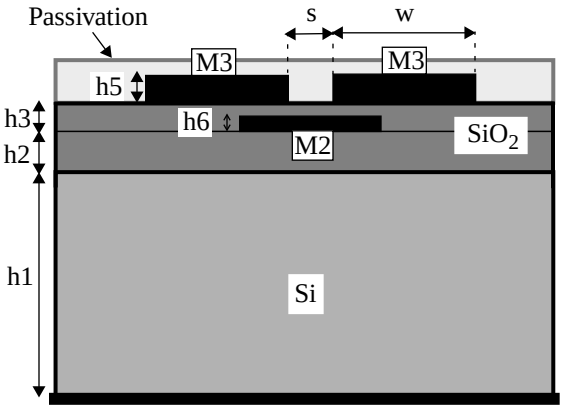

Fig. 4. Cross-sectional view of the inductor.

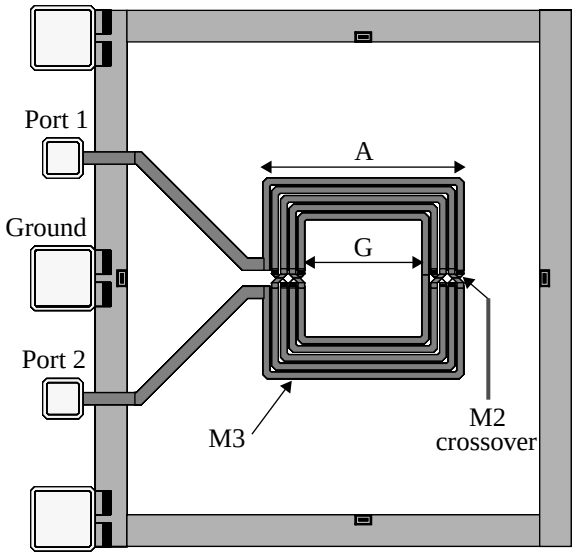

Fig. 5. Spiral inductor test structure layout.

Table 1. Substrate and metal parameters.

Parameter	Value
Oxide relative permittivity	$\varepsilon_r = 3.9$
Oxide thickness over M2	h3 - h6 = 1.3 μm
Oxide thickness below M2	h2 = 3.61 μm
Silicon relative permittivity	$\varepsilon_r = 11.7$
Silicon resistivity	$\rho = 15\ \Omega$–cm
Silicon thickness	h1 = 200 μm
Topmetal M3 resistivity	$\rho = 0.031\ \Omega$–μm
M3 thickness	h5 = 2.07 μm
M2 thickness	h6 = 0.84 μm

IV. Results and Discussion

Three-dimensional electromagnetic simulation (using HP-EEsof's Momentum) and experimental measurements were obtained for the 2-port spiral inductor. The results for the single-ended configuration were derived by grounding one of the ports (either Port1 or Port2) since the structure is symmetric. The response due to a differential excitation can be derived from 2-port S-parameter measurements using the relationship

$$S_D = S_{11} - S_{21} \tag{2}$$

The input impedances are determined from the 1-port S-parameters or the 2-port impedance matrix, as:

$$Z_{SE} = Z_{11} - \frac{Z_{12} \bullet Z_{21}}{Z_{22}} = Z_0\left(\frac{1+S_{11}}{1-S_{11}}\right) \tag{3}$$

and

$$Z_D = Z_{11} + Z_{22} - Z_{12} - Z_{21} = 2 \bullet Z_0\left(\frac{1+S_D}{1-S_D}\right) \tag{4}$$

where Z_0 is the system impedance (50 Ω).

Comparisons between experimental measurements and simulations for the input impedance and Q-factor (as defined by eq. 1) are shown in Figs. 6, 7 and 8. The series resistance at low frequencies (i.e., f < 0.5 GHz), as defined by r from the lumped element model of Figs. 2 and 3, was measured to be 7.3 Ω , while the simulation predicts 7.9 Ω . Measured and simulated low frequency inductances are 7.7 nH and 8.3 nH, respectively. At lower frequencies, the difference in Q between differential and single-ended excitations is not significant (<1%). This is because the shunt capacitive parasitic components do not affect the low frequency input impedance and hence, the two cases can be represented by a series L-r model. However, as the frequency increases, the difference between the input impedances becomes substantial; Z_D is much lower than Z_{SE} by an increasingly greater factor. This is caused by the lower substrate parasitics present in the differentially excited case, as previously described. The difference between Q-factors in the differential and single-ended cases, as shown in Fig. 8, illustrates this point. The peak in the Q-factor is a result of the shunt parasitics resonating with the inductance. Lower parasitics for differential excitation result in a higher peak Q-factor and broadening of the Q peak, when compared to the conventional single-ended connection.

For the single-ended excitation, the peak Q-factor is 6.6 at 1.6 GHz from both measurement and simulation. However, for a differential excitation, the resulting peak Q occurs at a higher frequency (2.5 GHz), with a value of 9.7 from measurement and 10.3 from simulation. This is a 47% increase in the measured peak Q between the differential and single-ended cases that can be realized without modification to the fabrication process. Achieving a comparable Q value in the single-ended connection would require an increase of approximately twice the top-metal thickness. At frequencies beyond the peak, an increase of greater than 50% can be achieved. It should be noted that Q values for the differential case, because they are greater in magnitude, are much more sensitive to slight variations in the measured or simulated input impedance. Thus, the relative effect of an error in either the measurement or simulation near the peak Q for the differential case is more pronounced. A slight increase in the topmetal thickness could account for part of the discrepancy between the measured and simulated performance. This would be consistent with the lower series resistance and inductance observed from the measurements when compared to the simulated values. The measured data shown is from a representative sample; several measurements were performed which gave the same results within a ±5% variation.

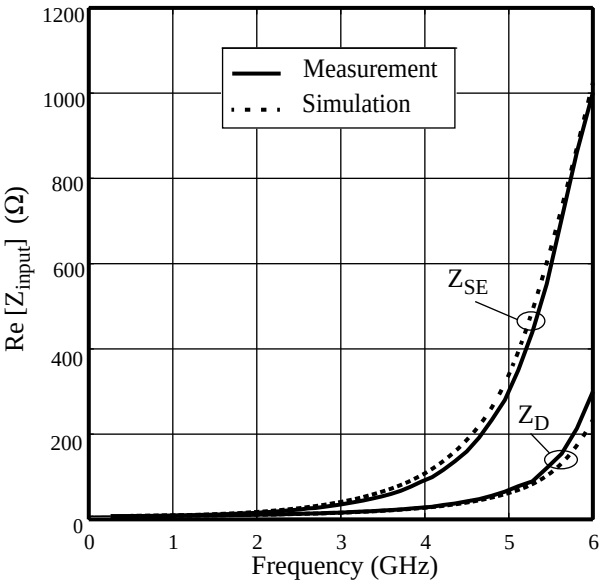

Fig. 6. Resistive Z_{SE} and Z_D.

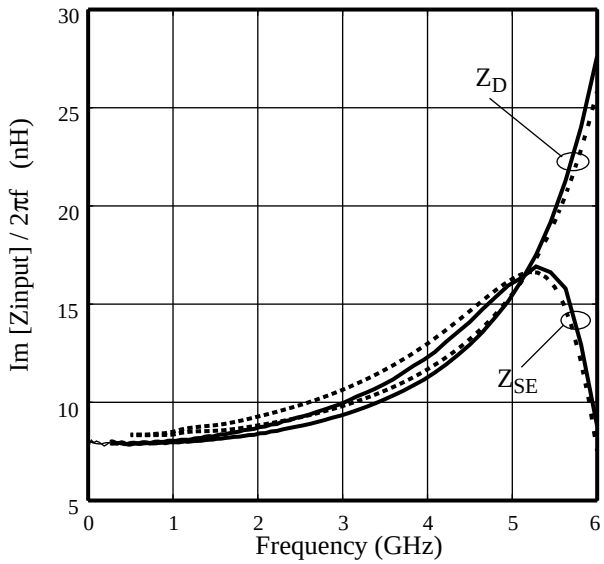

Fig. 7. Inductive Z_{SE} and Z_D.

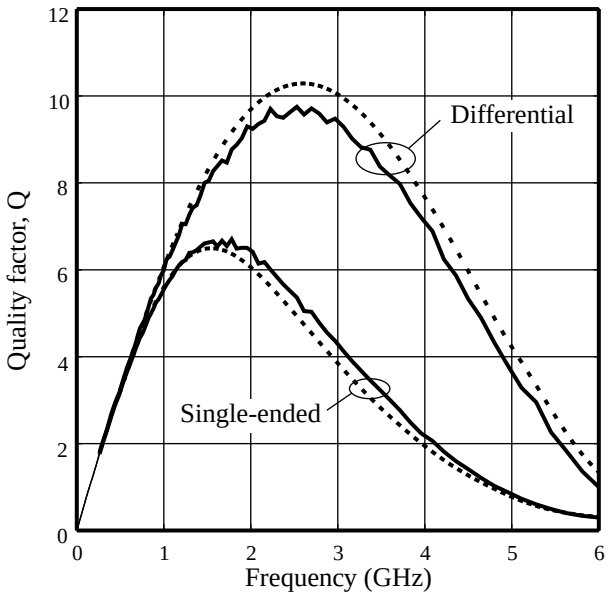

Fig. 8. Measured and simulated Q-factor.

Table 2 lists the parameters of a lumped-element model (see Fig. 9) that was fit over a broadband of frequency (500-6000MHz) for the inductor from the simulated data for both the single-ended and differential connections. The resistive parasitic element is 2.8 times higher for differential excitation, and the shunt capacitance is a small fraction of the single-ended case (C1: 38%, C2: 70%). The modified values for the lumped element models differ from the equivalent circuits shown in Figs. 2 and 3 due to the distributed nature of the actual inductor, which cannot be modeled accurately by a single lumped-element section for both one and two-port configurations.

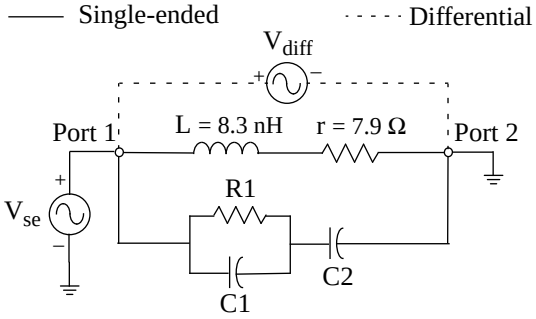

Fig. 9. Equivalent circuit model for both configurations.

Table 2. Lumped element parameter fitting.

Excitation	C1 (fF)	C2 (fF)	R1 (Ω)
Single-ended	135	162	358
Differential	95	62	1000

V. Conclusion

Higher peak Q-factor values and a wider operating bandwidth for monolithic inductors can be achieved by exciting a microstrip structure differentially. This could be exploited in many MMIC circuit applications, such as oscillators, mixers and amplifiers, where high-quality components are required. Measured and simulated results presented in this paper have validated the prediction of lower substrate parasitics that were made from a simplified lumped element model. The improvement in performance has been demonstrated for an inductor fabricated in a production silicon IC technology, however, these same results would apply to microstrip inductors fabricated on other substrates, such as GaAs.

Acknowledgements

This work was supported by Micronet and the Natural Sciences and Engineering Research Council of Canada (NSERC).

References

[1] J. R. Long and M. A. Copeland, "The Modeling, Characterization, and Design of Monolithic Inductors for Silicon RF ICs", *IEEE J. Solid-State Circuits*, Vol. 32, No. 3, March 1997, pp. 357-369.

[2] K. B. Ashby, I. A. Koullias, W. C. Finley, J. J. Bastek and S. Moinian, "High Q Inductors for Wireless Applications in a Complementary Silicon Bipolar Process", *IEEE J. Solid-State Circuits*, Vol. 31, No. 1, January 1996, pp. 4-9.

[3] J. N. Burghartz, M. Soyuer, K. A. Jenkins, M. Kies, M. Dolan, K. J. Stein, J. Malinowski and D. L. Harame, "Integrated RF Components in a SiGe Bipolar Technology", *IEEE J. Solid-State Circuits*, Vol. 32, No. 9, September 1997, pp. 1440-1445.

[4] M. Park, S. Lee, H. K. Yu, J. G. Koo and K. S. Nam, "High Q CMOS-Compatible Microwave Inductors using Double-Metal Interconnection Silicon Technology", *IEEE Microwave and Guided Wave Letters*, Vol. 7, No. 2, February 1997, pp. 45-47.

[5] J. Y.-C. Chang, A. A. Abidi and M. Gaitan, "Large Suspended Inductors on Silicon and Their Use in a 2-µm CMOS RF Amplifier", *IEEE Electron Device Letters*, Vol. 14, No. 5, May 1993, pp. 246-248.

[6] A. C. Reyes, S. M. El-Ghazali, S. J. Dorn, M. Dydyk, D. K. Schroder and H. Patterson, "Coplanar Waveguides and Microwave Inductors on Silicon Substrates", *IEEE Trans. Microwave Theory Tech.*, Vol. 43, No. 9, September 1995, pp. 2016-2022.

[7] H. Hasegawa, M. Furukawa and H. Yanai, "Properties of Microstrip Line on Si-SiO_2 System", *IEEE Trans. Microwave Theory Tech.*, Vol. 19, No. 11, November 1971, pp. 869-881.